Annals of Microbiology (2019) 69:377–394
https://doi.org/10.1007/s13213-018-1425-0

ORIGINAL ARTICLE

iTRAQ-based proteomic analysis of responses of *Lactobacillus plantarum* FS5-5 to salt tolerance

Mo Li[1] · Qianqian Wang[1] · Xuefei Song[1] · Jingjing Guo[1] · Junrui Wu[1] · Rina Wu[1]

Received: 26 August 2018 / Accepted: 20 December 2018 / Published online: 5 January 2019

Abstract

Lactobacillus plantarum FS5-5 (*L. plantarum* FS5-5) is a salt-tolerant probiotic strain, which had been isolated from northeast Chinese traditionally fermented *Dajiang*. We analyzed the underlying molecular mechanisms of *L. plantarum* FS5-5 after salt stress by isobaric tags for relative and absolute quantitation (iTRAQ)-based proteomics and bioinformatics analysis. *L. plantarum* FS5-5 was treated with low (1.5, 3.0, 4.0, and 5.0% (*w*/*v*) NaCl) and high (6.0, 7.0, and 8.0% (*w*/*v*) NaCl) salt stress. Differentially expression proteins (DEPs) of all groups were measured by quantitative proteomic approach of iTRAQ with LC–MS/MS. Furthermore, DEPs were identified by Mascot and GO, and bioinformatics analysis was conducted by KEGG. Thirty DEPs ($P < 0.05$) between low salt stress and control condition (0% (*w*/*v*) NaCl) were mapped and classified into nine functional groups; 122 DEPs ($P < 0.05$) between high salt stress and control condition were mapped and classified into 15 functional groups. In all groups, most proteins were involved in amino acid metabolism, carbohydrate metabolism, nucleotide metabolism, and ATP-binding cassette (ABC) transporter. We found that six proteins (*metS*, *GshAB*, *GshR3*, *PepN*, *GshR4*, and *serA*) involved in amino acid metabolism, three proteins (*I526_2330*, *Gpd*, and *Gnd*) involved in carbohydrate metabolism, and one protein (*N876_0118940*) involved in peptidoglycan hydrolysis were upregulated after salt stress. Conclusively, optimal *L. plantarum* FS5-5 growth was dependent on the collective action of different regulatory systems, with each system playing an important role in adapting to salt stress. There may be some relationship between the upregulated proteins of *L. plantarum* FS5-5 and salt stress.

Keywords Proteomic analysis · Salt stress · Lactic acid bacteria · iTRAQ

Introduction

Lactobacillus is a large group of lactic acid bacteria (LAB), which includes more than 150 different species. *Lactobacillus plantarum* (*L. plantarum*) is one of the most widespread *Lactobacillus* species and is commonly used in fermentation industry as the starter (Behera et al. 2018). During the fermentation process, *L. plantarum* forms organic acids, amino acids, small peptides, and other flavor compounds and generate peroxide and bacteriocins and other natural antibacterial substances, thus, imparting a special flavor, quality, and nutritional value to the fermented products. In addition, probiotic functions of *L. plantarum*, such as anti-oxidation, cholesterol-lowering, and immunity-enhancing, have been confirmed by a large number of researchers (Gill et al. 2000; Jones et al. 2012; Li et al. 2013). In the food industry, *L. plantarum* is commonly used as the starter for fermenting vegetables and dairy, meat, and soy products. However, *L. plantarum* is exposed to various stress conditions, such as temperature, acid, salt, starvation, osmotic pressure, and oxidative stress during the industrial fermentation and food processing (Li et al. 2012), and increasing attention has been paid to understand the adaption mechanisms of *L. plantarum* to these stressful conditions in recent years (Belfiore et al. 2013; Bengoa et al. 2018; Engelhardt et al. 2018).

Salt stress is an important challenge for *L. plantarum* in a variety of fermented foods. High salt concentration can damage the morphology and physiology of the cells. Therefore, adaptation to salt stress is important for *L. plantarum* for thriving and proliferating in their natural ecosystems and in industrial applications (Zhao et al. 2014). In recent years, increasing studies have been performed to determine the changes in

✉ Junrui Wu
junruiwu@126.com

✉ Rina Wu
wrn6956@163.com

[1] College of Food Science, Shenyang Agricultural University, Shenyang 110866, People's Republic of China

L. plantarum under salt stress (Zhao et al. 2014). *L. plantarum* manages thriving in a high osmotic pressure environment by activating various adaptation strategies. Some membrane proteins directly or indirectly regulate cell membrane permeability of salt ions, thereby regulating the osmotic pressure (Kleerebezem et al. 2003; Wang et al. 2011). The Na^+/H^+ antiporter on the plasma membrane regulates microbial efflux and influx of Na^+ and H^+ (Padan et al. 2005). The Na^+/H^+ antiporter is powered by a transmembrane proton electrochemical gradient that drives extracellular Na^+ to maintain intracellular Na^+ balance. Secondly, *L. plantarum* can also absorb or synthesize amino acids, small peptides, polyols, and disaccharides to maintain the balance of intracellular and extracellular osmotic pressure to resist various environmental stresses (Roberts 2005). Under high osmotic pressure, as enzymes that catabolize the compatible solute are inhibited, the compatible solute can accumulate in the cell at a high concentration, thus, leading to osmotic protection function. In addition, *L. plantarum* can maintain the balance of osmotic pressure by regulating the expression of some stress proteins and altering the composition of the cell membrane/cell wall (Romeo et al. 2001). Although a high number of studies have been conducted on the salt stress response of *L. plantarum*, the description of *L. plantarum* at the gene level under various salt concentration stresses is not much comprehensive.

Isobaric tags for relative and absolute quantitation (iTRAQ) is a new quantitative proteomic approach and has been widely used in the identification, characterization, and expression analysis of the proteins (Gao et al. 2017; Lin et al. 2017). Multiple peptides representing the same protein may be identified with iTRAQ, which affords higher confidence for both identification and quantification of the protein (Li et al. 2017).

L. plantarum FS5-5 (CGMCC no. 10331) is a salt-tolerant strain isolated from Northeast Chinese traditionally fermented *Dajiang*. The objectives of this study were to analyze the response of *L. plantarum* FS5-5 to salt stress (1.5, 3.0, 4.0, 5.0, 6, 7, and 8% (*w*/*v*) NaCl) at the protein and gene transcription levels by iTRAQ multidimensional coupled with liquid chromatography–tandem mass spectrometry (LC–MS/MS) proteomic approach. We propose that the results will provide an important molecular basis and reference information for future study of *L. plantarum* salt tolerance.

Materials and methods

Strains, growth conditions, and salt stress

L. plantarum FS5-5, isolated from Northeast Chinese traditionally fermented *Dajiang* in the Liaoning province of China, showed higher capacity to high salt tolerance based on our previous report (Song et al. 2016). For salt stress response analysis, the strain, which was freeze-dried and stored at − 80 °C, was reconstituted at 37 °C (optimum growth temperature for *L.plantarum* FS5-5) in de Man, Rogosa, and Sharpe medium (MRS) for 24 h, and this procedure was repeated three times. Bacterial suspension (1%; 10^6 colony forming units (CFU)/mL) was inoculated in MRS with 0, 1.5, 3.0, 4.0, 5.0, 6.0, 7.0, and 8.0% (*w*/*v*) NaCl and incubated at 37 °C to reach the exponential phase (at 6, 6, 6, 7, 8, 10, 13, and 18 h, respectively). Cell pellets were prepared by centrifugation at 4000 ×*g* at 4 °C for 10 min and washed three times with phosphate buffer. The final bacterial solution concentration reached 10^9 CFU/mL and was stored at − 80 °C until further use.

Transmission electron microscope (TEM) analysis

L. plantarum FS5-5 cells with 0, 1.5, 3.0, 4.0, 5.0, 6.0, 7.0, and 8.0% (*w*/*v*) NaCl were cultured at 37 °C to reach the exponential phase (6, 6, 6, 7, 8, 10, 13, and 18 h, respectively) and fixed in buffered 2.5% glutaraldehyde. Cells were collected after centrifugation at 4000 ×*g* at 4 °C for 10 min and washed three times with physiological saline to remove excess fixative. The cells were fixed in unbuffered 1% osmium tetroxide and washed with physiological saline. Then, the samples were dehydrated in ethanol at concentrations of 50, 70, 80, 90, and 95% and dehydrated in a graded series of acetone solutions and gradually impregnated in EPON resin with heat polymerization. Semi-thin survey sections were sliced with glass knives, stained with 1% phosphotungstic acid, and used to orient sections (Feliciano and Rivera 2016). Thin sections were viewed under a TEM (H-7650, Hitachi Ltd. Japan).

Protein extraction and quantification

Proteins were extracted according to a previously reported method (Xia et al. 2016) with slight modifications. Cells (500 μg) at the logarithmic stage of each NaCl concentration were mixed with 1 mL of lysis solution, comprised of 8-M urea solution (1 mL), 30-mM HEPES (1 mL), 1-mM phenylmethane sulfonyl fluoride (PMSF; 1 mL), 2-mM EDTA (1 mL), and 10-mM dithiothreitol (DTT; 1 mL), and the total protein was further lysed by ultrasonication (pulse on, 2 s; pulse off, 3 s; power 180 W), followed by centrifugation at 20,000 ×*g* for 30 min at 4 °C. The supernatant was collected, and DTT was added to the supernatant at a final concentration of 10 mM and incubated at 56 °C in water bath for 1 h. After removing the mixture from the water bath, iodoacetamide (IAM) was added rapidly to the mixture at a final concentration of 55 mM and incubated in darkness for 1 h. Next, acetone was added at four times the volume of the mixture, incubated at − 20 °C for 3 h, centrifuged at 20,000 ×*g* for 30 min at 4 °C, precipitate was collected, dissolution buffer (final triethyl ammonium bicarbonate (TEAB) concentration, 50%;

and final sodium dodecyl sulfate (SDS) concentration, 0.1%) was added to the precipitate, ultrasonic treatment was administered as mentioned above, and the mixture was centrifuged at 20,000 ×*g* for 30 min at 4 °C. The supernatant was collected, and protein concentration was quantified using the Bradford method (Braford 1976).

Protein digestion and iTRAQ labeling

The proteins extracted (100 μg) from each samples were digested with trypsin, and the peptide samples were lyophilized and labeled using the iTRAQ Reagent-8Plex Multiplex Kit (AB SCIEX, Foster City, CA, USA) according to the manufacturer's instructions. Each sample was tagged as follows: the sample without NaCl was labeled with tags 113, sample with 1.50% (*w*/*v*) NaCl was labeled with tags 114, sample with 3.0% (*w*/*v*) NaCl was labeled with tags 115, sample with 4.0% (*w*/*v*) NaCl was labeled with tags 116, sample with (*w*/*v*) 5.0% NaCl was labeled with tags 117, sample with 6.0% (*w*/*v*) NaCl was labeled with tags 118, sample with 7.0% (*w*/*v*) NaCl was labeled with tags 119, and sample with (*w*/*v*) 8.0% NaCl was labeled with tags 120.

Strong cation exchange (SCX) chromatography separation

The labeled peptide samples were preliminary separated by SCX chromatography (Luna SCX 100A, Phenomenex, USA) according to a previously reported method (Yang et al. 2017) with slight modifications. iTRAQ-labeled peptides were dissolved in ten times the volume of buffer A (25% (*v*/*v*) acetonitrile (ACN), 10-mM KH_2PO_4; pH 3.0) and centrifuged at 15,000 ×*g* for 10 min. The supernatant was collected and purified on SCX column. The peptide samples were eluted at a flow rate of 1 mL/min with a gradient of 0–5% buffer B (25% (*v*/*v*) ACN, 2-M KCl, and 10-mM KH_2PO_4; pH 3.0) for 1 min, 5–30% buffer B for 10 min, 30–50% buffer B for 5 min, 50% buffer B for 10 min, 50–100% buffer B for 5 min, and 100% buffer B for 10 min. The eluent was collected after 214 nm, mixed according to the peaks, and then desalted on strata-X C18 column (Phenomenex, Torrance, CA, USA) according to a previously reported method (Xia et al. 2016).

Nano LC–MS/MS analysis

The peptide samples were separated using Nano-LC (DIONEX, USA) with a C18 chromatography column (100 mm × 75 mm, 300 A, 5 μg, C18; Phenomenex, USA) equilibrated with buffer A (0.1% formic acid in Milli-Q water) according to a reported method (Yang et al. 2017) with slight modifications. The peptide samples were loaded onto the C18 chromatography column and eluted at a flow rate of 400 nL/min, with a gradient of 5% buffer B (0.1% formic acid in ACN) for 10 min, 5–30% buffer B for 30 min, 30–60% buffer B for 5 min, 60–80% buffer B for 3 min, 80% buffer B for 7 min, and finally 5% buffer B for 10 min. The Q Exactive mass spectrometer (Thermo Fisher Scientific, USA) was used for data acquisition and performed as previously reported (Yu et al. 2017).

Protein identification and quantification

Mascot version 2.3.0 (Matrix Science, Boston, MA, USA) and Proteome Discoverer version 1.4 (Thermo Scientific, USA) software packages were used for iTRAQ protein identification and quantification analysis. The obtained raw data files were searched against the 1578_UNI_Lactobac database (downloaded on August 7, 2015; number of sequences, 461,115). The search parameters of Mascot for protein identification were as follows: Fixed modification, carbamidomethyl (C); variable modification, oxidation (M), Gln → Pyro→Glu (N-term Q), iTRAQ 8 plex (K), iTRAQ 8 plex (Y), iTRAQ 8 plex (N-term); peptide tol, ± 15 ppm; MS/MS tol, ± 20 mmμ; max missed cleavages, 1; enzyme, trypsin. Quantification analysis for each SCX elution was further performed using Proteome Discoverer; the parameters of which were as follows: protein ratio type, median; minimum peptides, 1; normalization method, median; *P* value, < 0.05. An identified protein was considered significantly upregulated or downregulated in abundance if the fold change (FC) met the threshold criterion of an iTRAQ ratio of 1.2 ($P < 0.05$). *P* value was calculated according to the equations of Cox and Mann.

Bioinformatics analysis

The differentially expressed proteins were mapped to Gene Ontology (GO) terms (http://www.geneontology.org) for functional classification and Kyoto Encyclopedia of Genes and Genomes (KEGG) pathways (http://www.kegg.jp/) for predicting the main metabolic pathways.

qRT-PCR analysis

To yield more accurate and reliable quantitative results of genes, the most stable reference gene was selected from the five housekeeping genes (*16S rRNA*, *gapdh*, *gapB*, *dnaG*, and *gyrA*). The primers for housekeeping genes and target genes are listed in Table 1, and qRT-PCR was performed as previously reported (Wu et al. 2016). The $2^{-\Delta\Delta CT}$ method was used to calculate the relative changes in gene expression (Livak and Schmittgen 2001) by comparing the CT values for 1.5, 3.0, 4.0, 5.0, 6.0, 7.0, and 8.0% (*w*/*v*) NaCl cultures with the 0% (*w*/*v*) NaCl culture. All samples were measured in triplicates.

Table 1 Primer sequences for quantitative PCR

Genes	Putative function	Sequences	Product
16Sr RNA	16S ribosomal RNA	AAGGGTTTCGGCTCGTAAAA(F) TGCACTCAAGTTTCCCAGTT(R)	247
gapdh	Glyceraldehyde-3-phosphate dehydrogenase	CGTCGTATTATGGATTTAGG(F) GAGCTTGTGACTTAGCCTTG(R)	286
gapB	Glyceraldehyde-3-phosphate dehydrogenase	TCTTGACTGCAGATGACCGT(F) AGTTACCACCACGTACAGGG(R)	174
dnaG	DNA primase	CGCACCTAAGGATCAGCAAC(F) AGTTGGTAGTCGGTCTGGTG(R)	225
gyrA	DNA gyrase subunit A	TTTAAGTCGCAACACCGTGG(F) GATTCCTTTGGCCGTACGAC(R)	183
araT	Aminotransferase, class I/II	GTTTCAACCATCCGCCAGTT (F) TAGTGGACGCCGTACTTTGT (R)	218
mapB	Maltose phosphorylase	ACGGTCAGCACACAGTCATA (F) GGTTCAGGCGCTTATCTTCG(R)	175
guaC	GMP reductase	TTCGGTCGGTGTTAAGTCCA (F) AGCATTTTCAAGGTCGCGAA (R)	211
purH	Phosphoribosylaminoimidazole carboxamide formyltransferase/IMP cyclohydrolase	CTGAGAAGATGCACGCACTC (F) TGTCGGTTGGGTTACGGTAA (R)	239
pflF	Formate C-acetyltransferase	GTTGCTCACCAGAACATGCA (F) AGGTCCGTAGTAGTGCAACC (R)	174
carA	Carbamoyl-phosphate synthase small subunit	CCAGCTTTCCTTTGGTCACC (F) CCTTCAATGCTGCCGTCATT (R)	168
purB	Adenylosuccinate lyase	ATTTCCCACTCTTCTGCGGA (F) CACGAGACATCCCCGTATCA (R)	199
purA	Adenylosuccinate synthase	CTCAGGGAGTCATGCTGGAT (F) GAGTTCAGTTGGGAATGGGC (R)	179
pyrF	Orotidine-5′-phosphate decarboxylase	ATACAACGGTTCATGCTGCG (F) TCCCATGATTTGCTGGTCCT (R)	167
N876_0118940	Gamma-D-glutamate-meso-diaminopimelate muropetidase	CAAACATCGATGCCAGCTCA (F) ACCATATTGTCGCAGCGTTC (R)	158
metS	Methionyl-tRNA synthetase	TTGGGAAACTTGCTGAACCG (F) CCAAGGTGCCGTTTCATCAA (R)	234

Statistical analysis

Data analysis was performed using the SPSS version 19.0 statistical software (SPSS Inc., Chicago, IL, USA). To examine intrasample variation, mean and standard deviation (SD) were determined. Gene expression data were also analyzed using analysis of variance (ANOVA). A protein was considered differentially expressed when it exhibited a FC of > 1.2 or < 0.83 and P value of < 0.05.

Results

Morphological changes in salt tolerance

The morphological changes of *L. plantarum* FS5-5 in 0, 1.5, 3.0, 4.0, 5.0, 6.0, 7.0, and 8.0% (*w*/*v*) NaCl were clearly observed by TEM (Fig. 1). The cell wall of cells subjected to low salt stress under 1.5, 3.0, 4.0, and 5.0% (*w*/*v*) was separated, and some cells exhibited a clear cavity compared with cells under 0% (*w*/*v*) NaCl. The appearance of cells subjected to salt stress under 6.0, 7.0, and 8.0% (*w*/*v*) NaCl was significantly damaged compared with that of cells under 0% (*w*/*v*) NaCl. The results revealed that high salt concentration could alter the osmotic pressure of cells and lead to cell shrinkage and breakage.

Protein quantification and identification

Protein samples were quantified using the Bradford method, and the concentration of protein was 1.55 μg/μL with 0% NaCl, 1.07 μg/μL with 1.5% NaCl, 1.21 μg/μL with 3.0% NaCl, 1.47 μg/μL with 4.0% NaCl, 1.26 μg/μL with 5.0% NaCl, 1.07 μg/μL with 6.0% NaCl, 1.25 μg/μL with 7.0% NaCl, and 1.32 μg/μL with 8.0% NaCl. The total ion current diagram (Fig. 2) was searched against the 1578_UNI_Lactobac database by Mascot version 2.3.0 and Proteome Discoverer version 1.4 software. A total of 2056 proteins were specifically identified from 85,516 MS/MS spectra, and 11,215 peptides were identified using the false

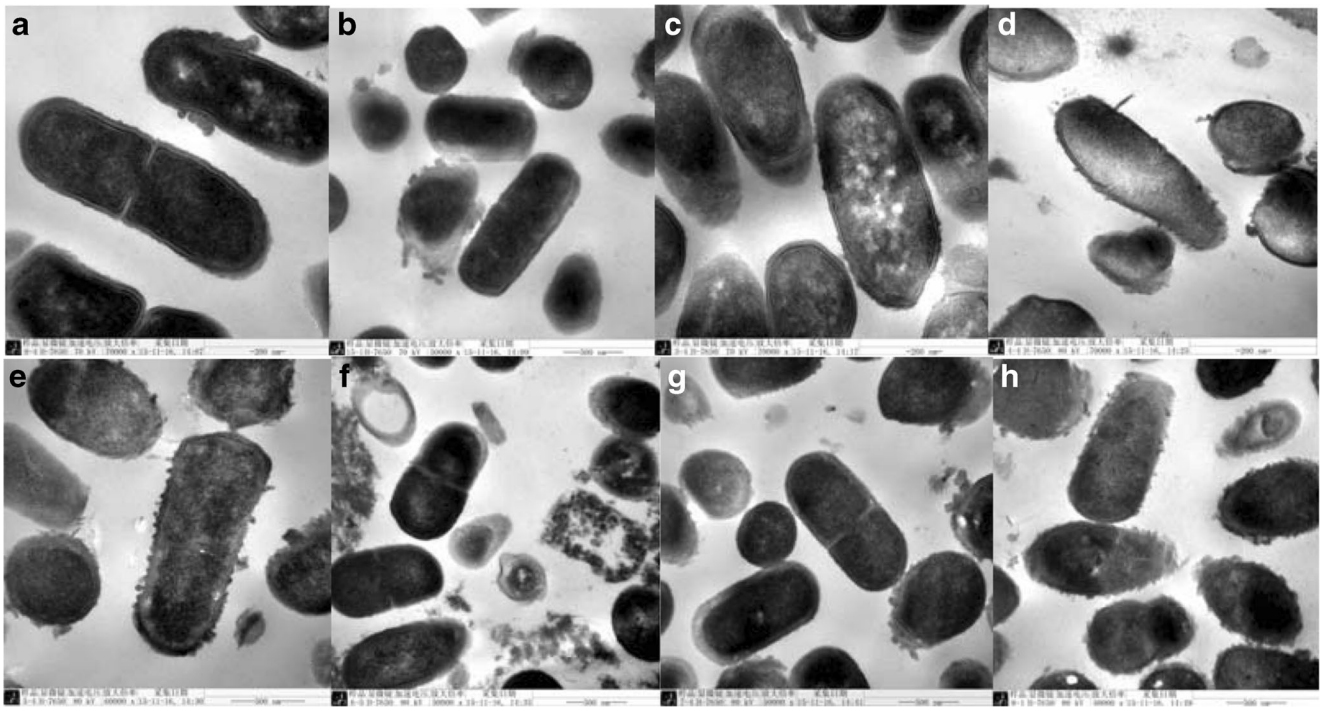

Fig. 1 TEM images of *L. plantarum* FS5-5 exposed in MRS medium at different NaCl concentrations. **a** 0.0%, **b** 1.5%, **c** 3.0%, **d** 4.0%, **e** 5.0%, **f** 6.0%, **g** 7.0%, **h** 8.0%

discovery rate (FDR) of < 1% as the cutoff. Significant differences in protein expression were determined using two criteria of "$P \leq 0.05$ and FC > 1.2 or FC < 0.83" for comparative analysis among the strains under 1.5, 3.0, 4.0, 5.0, 6.0, 7.0, and 8.0% (*w*/*v*) NaCl and under 0% (*w*/*v*) NaCl (Fig. 3).

From the results, we found that the amount of DEPs increased with the increase in NaCl concentration, implying that a high number of metabolic pathways are altered in *L. plantarum* FS5-5 to resist high salt stress.

Bioinformatics analysis of differential protein species identified by iTRAQ

The function and metabolic pathways of differential protein species were analyzed by mapping to GO terms and KEGG pathways. A total of 30 DEPs ($P < 0.05$) between low salt stress and control conditions were mapped and classified into nine functional groups (Fig. 4a), 122 DEPs ($P < 0.05$) between high salt stress and control condition were mapped and classified into 15 functional groups (Fig. 4b), and 22

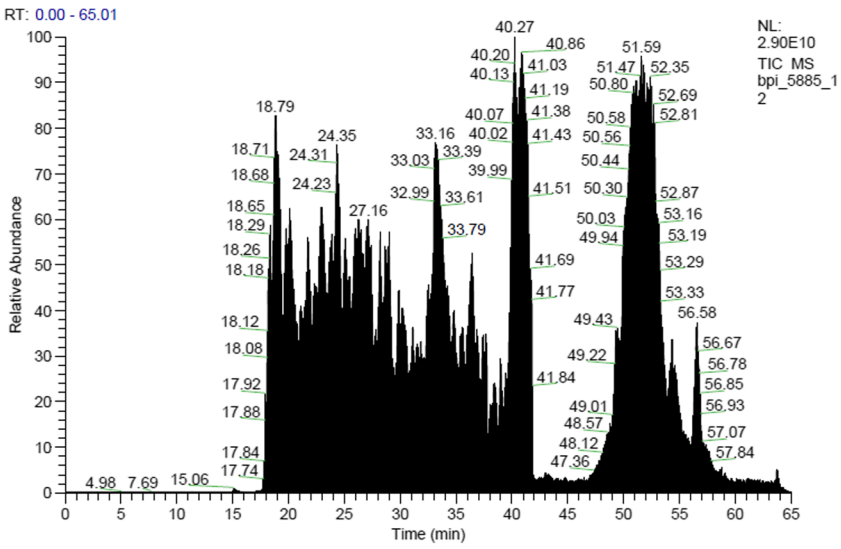

Fig. 2 The total ion current diagram. The x-axis represents the elution time. The y-axis represents the signal strength

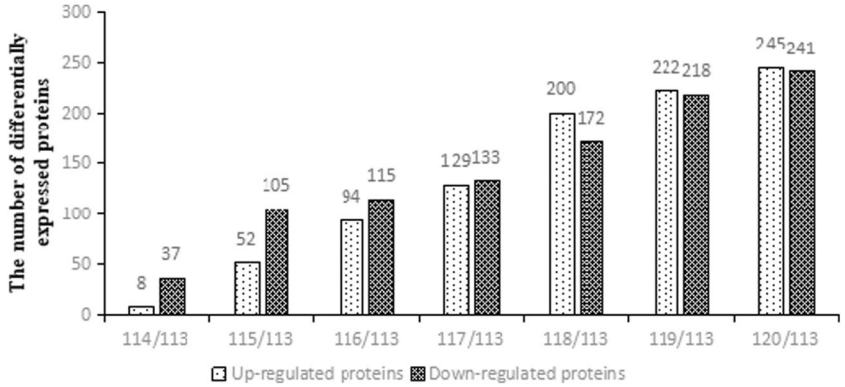

Fig. 3 Distribution of differently changed proteins. Proteins with corrected *P* values less than 0.05 and FCs larger than 1.20 or smaller than 0.83 were considered to be significantly differential; 114/113 represents the comparison between the samples with 1.5% (*w*/*v*) NaCl and the control samples; 115/113 represents the comparison between the samples with 3% (*w*/*v*) NaCl and the control samples; 116/113 represents the comparison between the samples with 4% (*w*/*v*) NaCl and the control samples; 117/113 represents the comparison between the samples with 5% (*w*/*v*) NaCl and the control samples; 118/113 represents the comparison between the samples with 6% (*w*/*v*) NaCl and the control samples; 119/113 represents the comparison between the samples with 7% (*w*/*v*) NaCl and the control samples; 120/113 represents the comparison between the samples with 8% (*w*/*v*) NaCl and the control samples

common DEPs ($P < 0.05$) in all high salt groups were mapped and classified into eight functional groups (Fig. 4c). The detailed information is provided in Tables 2–4. Most DEPs under low salt stress were involved in carbohydrate metabolism (26.67%), nucleotide metabolism (23.33%), ATP-binding cassette (ABC) transporter (20%), amino acid metabolism (10%), lipid metabolism (6.67%), vitamin metabolism (3.33%), phosphotransferase system (PTS; 3.33%), ribosomal protein (3.33%), and peptidoglycan hydrolysis (3.33%); most DEPs under high salt stress were involved in amino acid metabolism (17.21%), carbohydrate metabolism (17.21%), nucleotide metabolism (16.39%), ABC transporter (13.11%), ribosomal protein (9.02%), lipid metabolism (4.92%), replication and repair (6.56%), and PTS (3.28%). Moreover, most common DEPs were involved in nucleotide metabolism (31.82%), ABC transporter (27.27%), amino acid metabolism (9.09%),

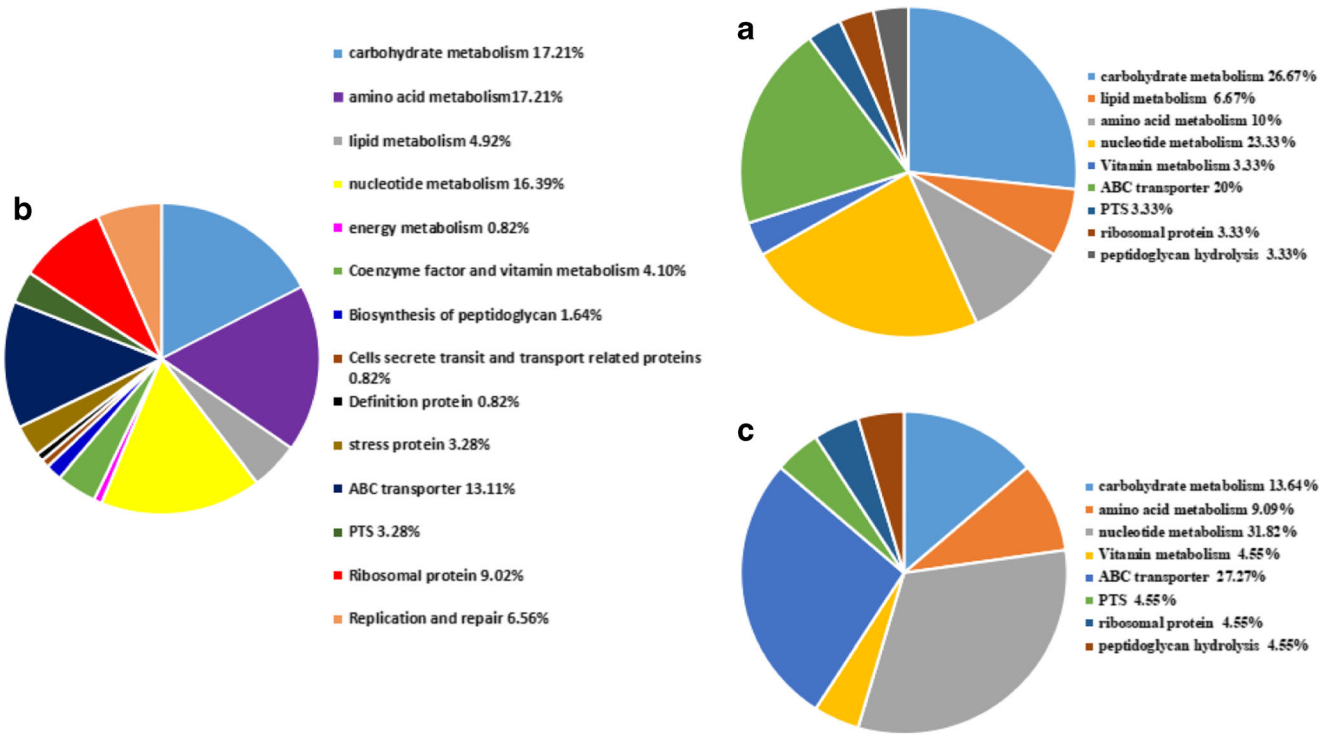

Fig. 4 Functional groups classification and proportion of differential protein species. Different colors represent different functional groups of differential protein species. **a** Differential protein species between low salt stress (1.5%, 3.0%, 4.0%, 5.0% *w*/*v*) NaCl) and control conditions. **b** Differential protein species between high salt stress (6.0%, 7.0%, 8.0% (*w*/*v*) NaCl) and control conditions. **c** Common differential protein species between all salt stress and control conditions

Table 2 The detailed information of differential protein species under high salt stress. Proteins with corrected *P* values less than 0.05 and FCs larger than 1.20 or smaller than 0.83 were considered to be significantly differential; 118/113 represents the comparison between the samples with 6% (*w*/*v*) NaCl and the control samples; 119/113 represents the comparison between the samples with 7% (*w*/*v*) NaCl and the control samples; 120/113 represents the comparison between the samples with 8% (*w*/*v*) NaCl and the control samples

No.	Protein name	Gene name	MW (kDa)[a]	*p*I[a]	Function	Fold change[b]		
						118/113	119/113	120/113
A0A023MDV6	Maltose phosphorylase	*mapB*	85.6	5.03	Carbohydrate metabolism	0.41	0.53	0.46
A0A023MCN6	Formate C-acetyltransferase	*pflF*	84.4	5.57	Carbohydrate metabolism	0.54	0.68	0.59
A0A023M9Z1	Fumarate hydratase class II	*fumC*	49.5	5.16	Carbohydrate metabolism	0.55	0.65	0.63
A0A023M826	Mannitol-1-phosphate 5-dehydrogenase	*mtlD*	43.2	5.27	Carbohydrate metabolism	0.57	0.64	0.79
A0A023M8J2	Mannose-specific phosphotransferase system, enzyme IIC	*I526_0522*	27.4	5.15	Carbohydrate metabolism	0.57	0.62	0.63
A0A023M9E0	Phosphotransferase system, mannose/fructose-specific component IIA	*I526_0521*	35.3	6.38	Carbohydrate metabolism	0.64	0.67	0.80
D7VDG0	PTS system, mannose/fructose/sorbose family, IID component	*pts9D*	34.3	9.39	Carbohydrate metabolism	0.64	0.64	0.72
A0A023MDE9	Aldehyde-alcohol dehydrogenase	*I526_2968*	94.5	6.79	Carbohydrate metabolism	0.65	0.72	0.65
A0A023MD66	N-acetylglucosamine and glucose PTS, EIICBA	*pts18CBA*	70.3	6.9	Carbohydrate metabolism	0.67	0.72	0.64
M4KGE1	Cps3J protein	*cps3J*	30.6	7.99	Carbohydrate metabolism	0.68	0.59	0.48
R9X3V8	Mannose-6-phosphate isomerase	*pmi*	35.9	5.4	Carbohydrate metabolism	0.70	0.65	0.73
M4KKC5	Glucose-6-phosphate 1-dehydrogenase	*gpd*	56.7	5.49	Carbohydrate metabolism	1.24	1.27	1.47
A1BND3	Putative pyruvate oxidase	*poxC*	63.8	5.29	Carbohydrate metabolism	1.26	1.41	1.42
qA0A023MC38	Acetyl-CoA carboxylase, biotin carboxylase subunit)	*accC1*	48.2	7.18	Carbohydrate metabolism	1.31	1.31	1.21
A0A023M9E2	Mannose PTS, EIIA	*pts10A*	15.3	4.63	Carbohydrate metabolism	1.34	1.40	1.26
A0A023MCE4	Phosphoglycerate mutase	*pgm*	24.9	7.15	Carbohydrate metabolism	1.40	1.44	1.51
D7V8V6	6-Phosphogluconate dehydrogenase, decarboxylating	*gnd*	52.9	5.3	Carbohydrate metabolism	1.48	1.41	1.83
D7VED2	Glycosyl hydrolase family 65 central catalytic domain protein	*map2*	102	6.6	Carbohydrate metabolism	1.62	2.19	1.61
D7VD75	NAD dependent epimerase/dehydratase family protein	*HMPREF0531_12098*	23.4	5.2	Carbohydrate metabolism	1.64	1.66	1.96
A0A023MA11	Beta-phosphoglucomutase	*pgmB*	23.6	5.36	Carbohydrate metabolism	2.07	1.78	2.01
A0A023MFR5	Alcohol dehydrogenase, zinc-containing	*I526_2330*	36.7	5.59	Carbohydrate metabolism	2.22	2.90	3.44
V7Z475	Dihydrodipicolinate synthase	*dapA*	18.3	8.75	Amino acid metabolism	0.14	0.32	0.28
D7VCV0	Aminotransferase, class I/II	*araT*	43	6.04	Amino acid metabolism	0.32	0.53	0.51
A0A023M934	Acetaldehyde dehydrogenase	*acdH*	48.6	6.8	Amino acid metabolism	0.69	0.76	0.58
A0A023MEE7	D-Alanine--poly(phosphoribitol) ligase subunit 1	*dltA*	56.1	4.98	Amino acid metabolism	0.73	0.60	0.66
M4KKX9	CblB protein	*cblB*	40.8	5.86	Amino acid metabolism	0.78	0.65	0.74
A0A023MF64	Ribosomal protein acetylating enzyme	*I526_1984*	21	5.17	Amino acid metabolism	0.81	0.73	0.70
A0A023MCV2	Aspartokinase	*thrA*	42.8	5.82	Amino acid metabolism	0.82	0.82	0.82

Table 2 (continued)

No.	Protein name	Gene name	MW (kDa)[a]	pI[a]	Function	Fold change[b]		
						118/113	119/113	120/113
A0A023MFJ8	Bifunctional glutamate--cysteine ligase/glutathione synthetase	*gshAB*	83	7.15	Amino acid metabolism	1.20	1.20	1.25
A0A023MC70	Succinate-semialdehyde dehydrogenase NADP	*gabD*	50.4	4.92	Amino acid metabolism	1.31	1.37	1.53
D7VFM8	Pyridine nucleotide-disulfide oxidoreductase	*gshR3*	48.2	5.39	Amino acid metabolism	1.32	1.36	1.38
F9UMD4	Membrane alanine aminopeptidase (Aminopeptidase N)	*pepN*	93.9	4.93	Amino acid metabolism	1.39	1.41	1.24
A0A023MDP9	S-Adenosylmethionine synthase	*metK*	42.6	4.94	Amino acid metabolism	1.39	1.50	1.67
U2JJ06	Proline iminopeptidase	*pepR1*	34.5	5.3	Amino acid metabolism	1.40	1.37	1.39
O08445	Alanine racemase	*alr*	40.7	5.59	Amino acid metabolism	1.43	1.52	1.64
Q76H90	Aspartate semialdehyde dehydrogenase	*asd*	38.2	5.78	Amino acid metabolism	1.46	1.23	1.25
Q88YI6	S-Ribosylhomocysteine lyase	*luxS*	17.4	6.52	Amino acid metabolism	1.52	1.44	1.52
A0A023MFL2	Phosphoglycerate dehydrogenase	*serA*	34.2	6.64	Amino acid metabolism	1.60	1.33	1.53
U2I3F6	Glutamate decarboxylase	*gadB*	53.3	5.97	Amino acid metabolism	1.72	2.53	2.50
T5JS50	Methionyl-tRNA synthetase	*metS*	8.3	4.42	Amino acid metabolism	1.77	2.15	2.5
A0A023MBV3	Succinyl-diaminopimelate desuccinylase	*dapE1*	40.8	5.1	Amino acid metabolism	2.02	1.89	2.63
A0A023MCW0	Glutathione reductase	*gshR4*	47.6	5.36	Amino acid metabolism	2.39	2.91	2.20
D7V979	FabA-like domain protein	*fabZ2*	15.1	7.46	Lipid metabolism	0.70	0.54	0.67
V7Z5W3	3-Ketoacyl-ACP reductase	*fabG2*	23.2	7.56	Lipid metabolism	0.72	0.55	0.62
A0A023MB83	Malonyl CoA-acyl carrier protein transacylase	*fabD*	33.2	5.44	Lipid metabolism	0.73	0.58	0.55
D7V978	Putative acetyl-CoA carboxylase, biotin carboxyl carrier protein	*accB*	16.3	4.55	Lipid metabolism	0.76	0.54	0.57
D7V973	3-Oxoacyl-[acyl-carrier-protein] synthase 3	*fabH*	35.3	7.25	Lipid metabolism	0.76	0.67	0.70
A0A023MC38	Acetyl-CoA carboxylase, biotin carboxylase subunit	*accC*	48.2	7.18	Lipid metabolism	1.31	1.31	1.21
V7Z294	Orotate phosphoribosyltransferase	*pyrE*	22.4	6.09	Nucleotide metabolism	0.22	0.25	0.31
A0A023MFH5	Carbamoyl-phosphate synthase small chain	*carA*	40	6.09	Nucleotide metabolism	0.24	0.26	0.27
D7VCT9	Dihydroorotate dehydrogenase	*pyrD*	31.2	6.64	Nucleotide metabolism	0.27	0.27	0.42
Q88SV6	Adenylosuccinate synthetase	*purA*	47.2	5.64	Nucleotide metabolism	0.29	0.34	0.48
P77883	Aspartate carbamoyltransferase	*pyrB*	34.7	6.54	Nucleotide metabolism	0.31	0.53	0.51
A0A023MEY2	Bifunctional purine biosynthesis protein PurH	*purH*	55.3	6.33	Nucleotide metabolism	0.37	0.39	0.48
Q88SV5	GMP reductase	*guaC*	35.4	6.87	Nucleotide metabolism	0.38	0.47	0.52
M4KK14	Dihydroorotase	*pyrC*	45.4	6.18	Nucleotide metabolism	0.38	0.42	0.44
P71479	Bifunctional protein PyrR 1	*pyrR1*	19.8	6	Nucleotide metabolism	0.39	0.44	0.53
V7Z7R9	Phosphoribosylaminoimidazole-succinocarboxamide synthase	*purC*	21.3	5.6	Nucleotide metabolism	0.41	0.47	0.53
P77888	Orotidine 5′-phosphate decarboxylase	*pyrF*	24.9	7.59	Nucleotide metabolism	0.45	0.40	0.39
A0A023MGM5	Adenylosuccinate lyase	*purB*	49	5.97	Nucleotide metabolism	0.48	0.62	0.71
Q88Z76	CTP synthase	*pyrG*	59.7	5.69	Nucleotide metabolism	0.63	0.59	0.57
Q88WR0	Uridine kinase	*udk*	24	5.67	Nucleotide metabolism	0.67	0.67	0.68
P59389	Bifunctional protein PyrR 2	*pyrR2*	19.3	7.42	Nucleotide metabolism	0.78	0.81	0.80
F9US18	Anaerobic ribonucleoside-triphosphate reductase	*nrdD*	83.7	7.84	Nucleotide metabolism	0.83	0.68	0.70
D7VBM3	RelA/SpoT family protein	*relA*	86.2	7.72	Nucleotide metabolism	1.26	1.21	1.27

Table 2 (continued)

No.	Protein name	Gene name	MW (kDa)[a]	pI[a]	Function	Fold change[b]		
						118/113	119/113	120/113
A0A023MBG1	Ribonucleotide-diphosphate reductase subunit beta	*nrdF*	39.1	4.61	Nucleotide metabolism	1.26	1.50	1.48
Q88V20	Non-canonical purine NTP pyrophosphatase	*lp_2267*	21.8	6.96	Nucleotide metabolism	1.43	1.47	1.64
F9UQB6	ADP-ribose pyrophosphatase	*lp_2183*	20.5	4.87	Nucleotide metabolism	1.48	1.48	1.67
A0A023M9W7	NADH dehydrogenase	*ndh1*	71.8	8.85	Energy metabolism	0.65	0.58	0.56
A0A023MDX1	Riboflavin biosynthesis protein RibBA	*I526_1205*	43.6	6.89	Coenzyme factor and vitamin metabolism	0.46	0.51	0.46
R9X1Q3	Cytidine/deoxycytidylate deaminase	*Lp16_1101*	29.2	8.13	Coenzyme factor and vitamin metabolism	0.51	0.66	0.55
V7Z2C5	Nicotinate phosphoribosyltransferase	*nadC*	40.2	6.33	Coenzyme factor and vitamin metabolism	0.60	0.63	0.65
A0A023M9Y3	Riboflavin biosynthesis protein	*I526_1702*	37	7.24	Coenzyme factor and vitamin metabolism	1.20	1.29	1.23
Q88Z44	Holo-[acyl-carrier-protein] synthase	*acpS*	13.2	6.55	Coenzyme factor and vitamin metabolism	1.66	2.20	2.23
A0A023M993	UDP-N-acetylmuramate-L-alanine ligase	*murC*	48.7	5.67	Biosynthesis of peptidoglycan	0.78	0.70	0.73
V7Z5P8	UDP-N-acetylglucosamine 1-Carboxyvinyltransferase	*murA*	41.6	5.68	Biosynthesis of peptidoglycan	0.79	0.81	0.77
V7Z492	Membrane protein	*N876_0123875*	16.4	9.86	Cells secrete transit and transport related proteins	0.61	0.61	0.55
A0A023MC04	D-Alanyl transfer protein DltD	*I526_1691*	48.6	9.76	Definition protein	0.70	0.60	0.71
U2HMA7	Universal stress protein	*uspA*	17.6	9.92	Stress protein	1.71	1.87	1.92
A0A023M9S1	Small heat shock protein	*hsp*	16	4.7	Stress protein	1.82	2.22	2.06
A0A023MBA8	Alkaline shock protein	*asp*	16.1	4.94	Stress protein	2.36	1.95	1.92
A0A023M8S1	General stress protein	*lp_1597*	15.8	5.06	Stress protein	2.38	1.95	1.88
A0A023M8Y1	ABC transporter, ATP-binding protein	*I526_0147*	33.8	8.5	ABC transporter	0.33	0.42	0.37
M4KLW8	Phosphate import ATP-binding protein PstB	*pstB1*	30.4	5.73	ABC transporter	0.35	0.38	0.36
A0A023M9I7	Glutamine ABC transporter, substrate binding and permease protein	*glnPH2*	52.2	9.64	ABC transporter	0.72	0.54	0.52
A0A023MB03	Maltose/maltodextrin ABC transporter, substrate binding protein	*malE*	45.6	9.69	ABC transporter	0.50	0.70	0.66
A0A023MCW7	Oligopeptide ABC transporter, permease protein	*I526_1074*	37.6	9.31	ABC transporter	0.62	0.57	0.54
A0A023M9K8	Glutamine ABC transporter, permease protein	*I526_0736*	23.8	9.09	ABC transporter	0.65	0.69	0.74
U2HNB3	Peptide ABC transporter substrate-binding protein	*N876_09685*	36.6	6.02	ABC transporter	0.74	0.66	0.59
A0A023M995	ABC transporter component	*I526_1232*	47.5	5.77	ABC transporter	0.77	0.63	0.67
A0A023MAZ6	Lipoprotein, peptide binding protein OppA-like protein	*I526_0648*	59.9	9.61	ABC transporter	0.74	0.57	0.62
A0A023MDM8	ABC-type dipeptide/oligopeptide/nickel transport system, ATPase component	*I526_1075*	39.7	5.87	ABC transporter	0.81	0.55	0.65
A0A023ME81	Glycine betaine/carnitine/choline ABC transporter, substrate binding protein	*I526_1355*	34.8	9.36	ABC transporter	1.26	1.29	1.28
A0A023MDL1	Glycine betaine/carnitine/choline ABC transporter, permease protein	*I526_1354*	22.4	8.4	ABC transporter	1.37	1.47	1.56
F9UNY1	Glycine betaine/carnitine/choline ABC transporter, ATP-binding protein	*opuA*	44.4	5.16	ABC transporter	1.43	1.39	1.43
R9X8D2	Glycine/betaine/carnitine ABC transporter, ATP-binding subunit(ProV)	*Lp16_F055*	43.9	6.06	ABC transporter	1.54	1.82	1.99
R9XAV7	Glycine/betaine/carnitine ABC transporter, substrate binding lipoprotein	*Lp16_F053*	33.5	10.04	ABC transporter	1.64	1.74	1.55
A0A023M8N2	ABC-type polar amino acid transport system, ATPase component	*I526_0667*	26.8	5.48	ABC transporter	0.55	0.55	0.60
A0A023MB66	Beta-glucosides PTS, EIIABC	*I526_0231*	69.5	8.24	PTS	0.39	0.44	0.43
A0A023MD66	N-Acetylglucosamine and glucose PTS, EIICBA	*I526_2056*	70.3	6.9	PTS	0.67	0.72	0.64

Table 2 (continued)

No.	Protein name	Gene name	MW (kDa)[a]	pI[a]	Function	Fold change[b]		
						118/113	119/113	120/113
A0A023MB66	Beta-glucosides PTS, EIIABC	*pts4ABC*	69.5	8.24	PTS	0.74	0.58	0.82
A0A023M9E2	Mannose PTS, EIIA	*I526_0526*	15.3	4.63	PTS	1.34	1.40	1.26
Q88XZ0	30S ribosomal protein S12	*rpsL*	15.2	11.25	Ribosomal protein	0.57	0.42	0.35
Q88WN3	50S ribosomal protein L27	*rpmA*	10.1	10.95	Ribosomal protein	0.62	0.61	0.58
Q88WU7	50S ribosomal protein L35	*rpmI*	7.4	12.04	Ribosomal protein	0.64	0.23	0.21
Q88VD4	30S ribosomal protein S20	*rpsT*	9.1	10.52	Ribosomal protein	0.67	0.58	0.61
Q88WK6	50S ribosomal protein L28	*rpmB*	7	11.91	Ribosomal protein	0.71	0.43	0.44
Q88XY2	30S ribosomal protein S19	*rpsS*	10.3	9.82	Ribosomal protein	0.74	0.58	0.82
U2I5Q9	50S ribosomal protein L30	*N876_10145*	4.4	8.69	Ribosomal protein	0.77	0.67	0.82
Q88XY3	50S ribosomal protein L2	*rplB*	30.2	10.55	Ribosomal protein	0.77	0.62	0.63
Q88YW7	50S ribosomal protein L7/L12	*rplL*	12.6	4.48	Ribosomal protein	0.79	0.70	0.79
Q88XW7	50S ribosomal protein L15	*rplO*	15.3	10.64	Ribosomal protein	0.82	0.79	0.78
Q88YX4	50S ribosomal protein L33	*rpmG*	5.7	9.6	Ribosomal protein	1.58	2.24	2.55
A0A023MFT5	Ribonuclease H	*I526_2100*	32.6	9.85	Replication and repair	1.20	1.27	1.21
Q88UZ4	Protein RecA	*recA*	40.6	5.72	Replication and repair	1.26	1.71	2.05
A0A023MA12	DNA ligase	*ligA*	74.4	5.24	Replication and repair	1.34	1.36	1.58
U2WPA2	Single-stranded DNA-binding protein	*N644_0531*	20.9	5.12	Replication and repair	1.42	1.82	2.13
Q88YI8	UvrABC system protein B	*uvrB*	76.1	5.2	Replication and repair	1.44	1.91	2.39
A0A023M8F3	DEAD-box ATP-dependent RNA helicase CshA	*cshA*	59	9.55	Replication and repair	0.78	0.68	0.81
A0A023MDU1	Chaperone protein DnaK	*dnaK*	66.7	4.84	Replication and repair	0.78	0.61	0.57
M4KFD8	Ribonuclease R	*rnr*	90.7	6.21	Replication and repair	0.81	0.78	0.73
V7Z4U6	Gamma-D-glutamate-meso-diaminopimelate muropeptidase	*N876_0118940*	31.9	8.84	Peptidoglycan hydrolysis	1.56	1.50	1.87

[a] Theoretical values of molecular weight and isoelectric point

Fold change: average ratio from two biological replicates (treatments/controls) by iTRAQ study. A protein species was considered differentially accumulated as it exhibited a fold-change > 1.2 or fold-change < 0.83 and a *P* value < 0.05

carbohydrate metabolism (13.64%), vitamin metabolism (4.55%), ribosomal protein (4.55%), and PTS (4.55%).

From the results, we found that most DEPs were involved in amino acid, carbohydrate, and nucleotide metabolism, indicating that *L. plantarum* FS5-5 resistance to salt stress was closely related to these metabolic pathways.

Transcriptional expression analysis by qRT-PCR

The stability of the five housekeeping genes was evaluated by the $2^{-\Delta\Delta CT}$ method. The results are shown in Table 5. There was a certain correlation between the expression of *gapdh*, *gapB*, *dnaG*, and *gyrA* and salt stress ($P < 0.05$), but *16S rRNA* showed higher stability than other housekeeping genes ($P > 0.05$). Therefore, *16S rRNA* was selected as the internal reference gene for this experiment.

To determine whether the significant changes observed in specific proteins under high salt stress also occurred at the level of gene expression, qRT-PCR was performed to evaluate the mRNA levels of the proteins whose expression changed significantly. The results are shown in Fig. 5. The gene expression of *N876_0118940*, involved in peptidoglycan hydrolysis, and *metS*, involved in amino acid metabolism, was upregulated ($P < 0.05$) in cells at all NaCl levels, except for *metS* at 7.0% (*w*/*v*) NaCl. However, the mRNA levels of *araT*, involved in amino acid metabolism, in cells at all NaCl levels were repressed ($P < 0.05$), except at 5.0% (*w*/*v*) NaCl. The mRNA levels of *carA* (carbamoyl-phosphate synthase small subunit), *purB* (adenylosuccinate lyase), *purA* (adenylosuccinate synthase), *guaC* (GMP reductase), *purH* (phosphoribosylaminoimidazolecarboxamide formyltransferase/IMP cyclohydrolase), and *pyrF* (orotidine-5′-phosphate decarboxylase), involved in nucleotide metabolism, were repressed at all NaCl levels ($P < 0.05$), except for *purH* at 1.5% (*w*/*v*) NaCl. The mRNA levels of *mapB* and *pflF*, involved in carbohydrate metabolism, were repressed at all NaCl levels ($P < 0.05$). The results revealed that the mRNA expression of selected

Table 3 The information list of changed expression proteins under the low NaCl concentrations. Proteins with corrected *p* values less than 0.05 and fold changes larger than 1.20 or smaller than 0.83 were considered to be significantly differential; 114/113 represents the comparison between the samples with 1.5% (*w*/*v*) NaCl and the control samples; 115/113 represents the comparison between the samples with 3% (*w*/*v*) NaCl and the control samples; 116/113 represents the comparison between the samples with 4% (*w*/*v*) NaCl and the control samples; 117/113 represents the comparison between the samples with 5% (*w*/*v*) NaCl and the control samples

No.	Protein name	Gene name	MW (kDa)[a]	*p*I[a]	Function	Fold change[b]			
						114/113	115/113	116/113	117/113
A0A023MDV6	Maltose phosphorylase	*mapB*	85.6	5.03	Carbohydrate metabolism	0.50	0.33	0.34	0.36
A0A023MCN6	Formate C-acetyltransferase	*pflF*	84.4	5.57	Carbohydrate metabolism	0.77	0.60	0.59	0.63
A0A023M9Z4	Malate dehydrogenase	*mae*	59.5	4.89	Carbohydrate metabolism	0.70	0.67	0.70	0.79
A0A023MA62	Pyruvate dehydrogenase complex, E2 component, dihydrolipoamide S-acetyltransferase	*pdhC*	46.6	5.15	Carbohydrate metabolism	0.73	0.55	0.55	0.64
A0A023MBC5	Probable D-serine dehydratase	*dsdA*	47.6	5.95	Carbohydrate metabolism	0.7	0.54	0.52	0.66
A0A023MF20	6-Phospho-beta-glucosidase Glycosyl Hydrolase family 1	*I526_2248*	54.7	5.29	Carbohydrate metabolism	0.77	0.66	0.70	0.79
A0A023MCC8	Dihydrolipoyl dehydrogenase	*I526_1811*	49.9	5.45	Carbohydrate metabolism	0.79	0.61	0.70	0.73
A0A023M826	Mannitol-1-phosphate 5-dehydrogenase	*mtlD*	43.2	5.27	Carbohydrate metabolism	0.81	0.55	0.57	0.59
A0A023MA94	Dihydroxyacetone kinase phosphatase domain-containing protein	*dak2*	20	4.86	Lipid metabolism	0.68	0.46	0.57	0.58
D7V7W5	Dihydroxyacetone kinase	*dhaK*	36.1	4.96	Lipid metabolism	0.75	0.59	0.60	0.62
D7VCV0	Aminotransferase, class I/II	*araT*	43	6.04	Amino acid metabolism	0.34	0.29	0.30	0.33
A0A023MFH5	Carbamoyl-phosphate synthase small chain	*carA*	40	6.09	Amino acid metabolism	0.80	0.58	0.57	0.64
T5JS50	Methionyl-tRNA synthetase	*metS*	8.3	4.42	Amino acid metabolism	1.29	1.83	1.97	2.04
Q88SV5	GMP reductase	*guaC*	35.4	6.87	Nucleotide metabolism	0.69	0.37	0.49	0.57
A0A023MEY2	Bifunctional purine biosynthesis protein PurH	*purH*	55.3	6.33	Nucleotide metabolism	0.72	0.46	0.51	0.64
A0A023MGM5	Adenylosuccinate lyase	*purB*	49	5.97	Nucleotide metabolism	0.82	0.55	0.65	0.70
Q88SV6	Adenylosuccinate synthetase	*purA*	47.2	5.64	Nucleotide metabolism	0.82	0.36	0.51	0.56
V7Z294	Orotate phosphoribosyltransferase	*pyrE*	22.4	6.09	Nucleotide metabolism	0.75	0.52	0.50	0.55
A0A023MFH5	Carbamoyl-phosphate synthase small chain	*carA*	40	6.09	Nucleotide metabolism	0.80	0.58	0.57	0.64
P77888	Orotidine 5′-phosphate decarboxylase	*pyrF*	24.9	7.59	Nucleotide metabolism	0.82	0.61	0.60	0.65
V7Z2C5	Nicotinate phosphoribosyltransferase	*nadC*	40.2	6.33	Vitamin metabolism	0.76	0.64	0.65	0.73
A0A023M8N2	ABC-type polar amino acid transport system, ATPase component	*I526_0667*	26.8	5.48	ABC transporter	0.71	0.58	0.51	0.54
A0A023MB03	Maltose/maltodextrin ABC transporter, substrate binding protein	*malE*	45.6	9.69	ABC transporter	0.71	0.45	0.52	0.58
A0A023M9I7	Glutamine ABC transporter, substrate binding and permease protein	*glnPH2*	52.2	9.64	ABC transporter	0.72	0.54	0.52	0.59
A0A023M8Y1	ABC transporter, ATP-binding protein	*I526_0147*	33.8	8.5	ABC transporter	0.74	0.40	0.47	0.46
U2HNB3	Peptide ABC transporter substrate-binding protein	*N876_09685*	36.6	6.02	ABC transporter	0.77	0.73	0.80	0.74
A0A023M995	ABC transporter component	*I526_1232*	47.5	5.77	ABC transporter	0.82	0.69	0.71	0.67
A0A023MB66	Beta-glucosides PTS, EIIABC	*pts4ABC*	69.5	8.24	PTS	0.75	0.49	0.48	0.41
Q88XY2	30S ribosomal protein S19	*rpsS*	10.3	9.82	ribosomal protein	0.66	0.52	0.36	0.40

Table 3 (continued)

No.	Protein name	Gene name	MW (kDa)[a]	*pI*[a]	Function	Fold change[b]			
						114/113	115/113	116/113	117/113
V7Z4U6	Gamma-D-glutamate-meso-diaminopimelate muropeptidase	*N876_0118940*	31.9	8.84	peptidoglycan hydrolysis	1.25	1.42	1.53	1.79

[a] Theoretical values of molecular weight and isoelectric point

[b] Fold change: average ratio from two biological replicates (treatments/controls) by iTRAQ study. A protein species was considered differentially accumulated as it exhibited a fold-change > 1.2 or fold-change < 0.83 and a *P* value < 0.05

genes was almost consistent with the expression of the corresponding proteins.

Discussion

Proteins involved in amino acid metabolism

GshAB, which plays an important role in the biosynthesis and metabolism of glutathione, not only shows the catalysis as GshA but also shows catalytic effect as GshB and finally generates GSH. GSH plays important roles in bacterial cells, such as protecting proteins and DNA from oxidative damage and promoting transmembrane transport of amino acids. Moreover, GSH also can be converted to reduced glutathione by reductase (such as *GshR3* and *GshR4*) and aminopeptidase (such as *PepN*). The reduced glutathione not only can protect cells from oxidative damage but also can alleviate cell toxicity and stress damage (Vila Sanjurjo et al. 2004). In this study, *GshAB*, *GshR3*, *PepN*, and *GshR4* were overexpressed ($P < 0.05$) in *L. plantarum* FS5-5 in response to high salt stress but remained unaltered in response to low salt stress. In particular, *GshR4* was overexpressed by two-fold in bacteria at 6.0, 7.0, and 8.0% (*w*/*v*) NaCl than that in cells at 0% (*w*/*v*) NaCl. A previous study has shown that GSH protects *Lactococcus lactis* from osmotic stress (Zhang et al. 2010). Similarly, overexpression of glutathione reductase and aminopeptidase (*GshAB*, *GshR3*, and *GshR4* and *PepN*, respectively) may regulate the content of glutathione and reduced glutathione to protect *L. plantarum* FS5-5 from salt stress damage. Glutathione reductase can oxidize glutathione (GSSG) to glutathione catalyzed (GSH), which plays important roles in cellular antioxidant mechanisms. Previous studies have demonstrated that GSH protects cells from various environmental stresses, such as osmotic pressure, oxidative, and acid stress (Zhang et al. 2010; Zou et al. 2014; Wang 2015). It can be speculated that high salt concentration can induce the expression of *GshAB*, *GshR3*, *PepN*, and *GshR4*, thereby protecting *L. plantarum* FS5-5 from salt or other adverse environmental factors.

Proteins involved in carbohydrate metabolism

Carbohydrate metabolism is an important process for microbes as it provides the necessary energy for metabolism and significantly supports complete growth (Li et al. 2017a, 2017b). Glycolysis, as the main form of carbohydrate metabolism, provides energy to LAB under anaerobic conditions (Veith et al. 2017). *pgmB* (beta-phosphoglucomutase), which encodes a phosphoglucomutase, can catalyze the interconversion of D-glucose 1-phosphate (G1P) and D-glucose 6-phosphate (G6P) to yield beta-D-glucose 1,6-(bis) phosphate (beta-G16P) as an intermediate. Furthermore, *pgmB* plays a key role in the regulation of the flow of carbohydrate intermediates in glycolysis and the formation of the sugar nucleotide UDP-glucose. In this study, *pgmB* expression was upregulated ($P < 0.05$) in response to high salt stress but remained unaltered in response to low salt stress. Under high salt stress, *L. plantarum* FS5-5 may coordinate the supply of intracellular capacity and increase cell growth by upregulating the expression of *pgmB*.

The pentose phosphate pathway is also one of the major pathways for carbohydrate metabolism (Kovářová and Barrett 2016). In the present study, glucose 6-phosphate dehydrogenase (Gpd) and glucose 6-phosphate decarboxylase (Gnd) were both over-expressed in *L. plantarum* FS5-5 in response to 6.0, 7.0, and 8.0% (*w*/*v*) NaCl stress but remained unaltered in response to low salt stress. In the pentose phosphate pathway, Gpd catalyzes glucose 6-phosphate to produce phosphogluconate and generate NADPH; Gnd catalyzes glucose 6-phosphate to produce D-ribulose-5-phosphate, which is one of the major components of nucleotides and its important coenzymes, and NADPH to produce ribose-5-phosphate (Shi et al. 2009). These sugar phosphates are needed for the biosynthesis of nucleotides and coenzymes, and these compounds perhaps could be involved in the mechanism of *L. plantarum* FS5-5 response to salt stress.

Proteins involved in fatty acid metabolism

The adaptation of *L. plantarum* FS5-5 to high salinity is also accompanied by rearrangements in either the

Table 4 The information list of changed expression proteins under all NaCl concentrations. Proteins with corrected *P* values less than 0.05 and fold changes larger than 1.20 or smaller than 0.83 were considered to be significantly differential; 114/113 represents the comparison between the samples with 1.5% (*w*/*v*) NaCl and the control samples; 115/113 represents the comparison between the samples with 3% (*w*/*v*) NaCl and the control samples; 116/113 represents the comparison between the samples with 4% (*w*/*v*) NaCl and the control samples; 117/113 represents the comparison between the samples with 5% (*w*/*v*) NaCl and the control samples; 118/113 represents the comparison between the samples with 6% (*w*/*v*) NaCl and the control samples; 119/113 represents the comparison between the samples with 7% (*w*/*v*) NaCl and the control samples; 120/113 represents the comparison between the samples with 8% (*w*/*v*) NaCl and the control samples

No.	Protein name	Gene name	MW (kDa)[a]	*p*I[a]	Function	Fold change[b]						
						114/113	115/113	116/113	117/113	118/113	119/113	120/113
A0A023MDV6	Maltose phosphorylase	*mapB*	85.6	5.03	Carbohydrate metabolism	0.50	0.33	0.34	0.36	0.41	0.53	0.46
A0A023MCN6	Formate C-acetyltransferase	*pflF*	84.4	5.57	Carbohydrate metabolism	0.77	0.60	0.59	0.63	0.54	0.68	0.59
A0A023M826	Mannitol-1-phosphate 5-dehydrogenase	*mtlD*	43.2	5.27	Carbohydrate metabolism	0.81	0.55	0.57	0.59	0.57	0.64	0.79
D7VCV0	Aminotransferase, class I/II	*araT*	43	6.04	Amino acid metabolism	0.34	0.29	0.30	0.33	0.32	0.29	0.37
T5JS50	Methionyl-tRNA synthetase	*metS*	8.3	4.42	Amino acid metabolism	1.29	1.83	1.97	2.04	1.77	2.15	2.5
Q88SV5	GMP reductase	*guaC*	35.4	6.87	Nucleotide metabolism	0.69	0.37	0.49	0.57	0.38	0.47	0.52
A0A023MEY2	Bifunctional purine biosynthesis protein	*purH*	55.3	6.33	Nucleotide metabolism	0.72	0.46	0.51	0.64	0.37	0.39	0.48
A0A023MGM5	Adenylosuccinate lyase	*purB*	49	5.97	Nucleotide metabolism	0.82	0.55	0.65	0.70	0.48	0.62	0.71
Q88SV6	Adenylosuccinate synthetase	*purA*	47.2	5.64	Nucleotide metabolism	0.82	0.36	0.51	0.56	0.29	0.34	0.48
V7Z294	Orotate phosphoribosyltransferase	*pyrE*	22.4	6.09	Nucleotide metabolism	0.75	0.52	0.50	0.55	0.22	0.25	0.31
A0A023MFH5	Carbamoyl-phosphate synthase small chain	*carA*	40	6.09	Nucleotide metabolism	0.80	0.58	0.57	0.64	0.28	0.26	0.27
P77888	Orotidine 5′-phosphate decarboxylase	*pyrF*	24.9	7.59	Nucleotide metabolism	0.82	0.61	0.60	0.65	0.45	0.40	0.39
V7Z2C5	Nicotinate phosphoribosyltransferase	*nadC*	40.2	6.33	Vitamin metabolism	0.76	0.64	0.65	0.73	0.60	0.63	0.65
A0A023M8N2	ABC-type polar amino acid transport system, ATPase component	*I526_0667*	26.8	5.48	ABC transporter	0.71	0.58	0.51	0.54	0.55	0.55	0.60
A0A023MB03	Maltose/maltodextrin ABC transporter, substrate binding protein	*malE*	45.6	9.69	ABC transporter	0.71	0.45	0.52	0.58	0.50	0.70	0.66
A0A023M9I7	Glutamine ABC transporter, substrate binding and permease protein	*glnPH2*	52.2	9.64	ABC transporter	0.72	0.54	0.52	0.59	0.59	0.58	0.58
A0A023M8Y1	ABC transporter, ATP-binding protein	*I526_0147*	33.8	8.5	ABC transporter	0.74	0.40	0.47	0.46	0.33	0.42	0.37
U2HNB3	Peptide ABC transporter substrate-binding protein	*N876_09685*	36.6	6.02	ABC transporter	0.77	0.73	0.80	0.74	0.74	0.66	0.59
A0A023M995	ABC transporter component	*I526_1232*	47.5	5.77	ABC transporter	0.82	0.69	0.71	0.67	0.77	0.63	0.67
A0A023MB66	Beta-glucosides PTS, EIIABC	*pts4ABC*	69.5	8.24	PTS	0.75	0.49	0.48	0.41	0.39	0.44	0.43
Q88XY2	30S ribosomal protein S19	*rpsS*	10.3	9.82	Ribosomal protein	0.66	0.52	0.36	0.40	0.74	0.58	0.82
V7Z4U6	Gamma-D-glutamate-meso-diaminopimelate muropeptidase	*N876_0118-940*	31.9	8.84	Peptidoglycan hydrolysis	1.25	1.42	1.53	1.79	1.56	1.50	1.87

[a] Theoretical values of molecular weight and isoelectric point

[b] Fold change: average ratio from two biological replicates (treatments/controls) by iTRAQ study. A protein species was considered differentially accumulated as it exhibited a fold-change > 1.2 or fold-change < 0.83 and a *P* value < 0.05

composition or structure of the cell envelope. In particular, lipid and fatty acid composition of the cytoplasmic membrane is affected. Malonyl CoA, an important precursor in the biosynthesis of fatty acids, is converted

Table 5 Fold change in the gene expression of housekeeping genes under different salt concentrations

Gene	Fold change in gene expression								*P* value
	0% (*w*/*v*)	1.5% (*w*/*v*)	3% (*w*/*v*)	4% (*w*/*v*)	5% (*w*/*v*)	6% (*w*/*v*)	7% (*w*/*v*)	8% (*w*/*v*)	
16S rRNA	1	1.160 ± 0.077	1.171 ± 0.129	1.183 ± 0.035	1.189 ± 0.143	1.204 ± 0.066	1.220 ± 0.119	1.252 ± 0.104	0.081
gapdh	1	1.201 ± 0.019	1.240 ± 0.174	1.299 ± 0.031	1.300 ± 0.053	1.418 ± 0.010	1.574 ± 0.183	1.420 ± 0.184	0.009*
gapB	1	1.106 ± 0.144	1.137 ± 0.132	1.179 ± 0.007	1.232 ± 0.238	1.300 ± 0.363	1.398 ± 0.037	1.419 ± 0.175	0.017*
dnaG	1	1.399 ± 0.272	1.389 ± 0.290	1.430 ± 0.188	1.811 ± 0.163	2.126 ± 0.279	2.470 ± 0.247	2.682 ± 0.300	0.001*
gyrA	1	1.353 ± 0.044	1.426 ± 0.176	1.592 ± 0.020	1.701 ± 0.244	1.849 ± 0.355	2.409 ± 0.284	2.593 ± 0.308	0.004*

Data are presented as the mean ± standard deviation (SD) of triplicate experiments

*Significant difference ($P < 0.05$) of fold change in gene expression under different salt concentrations. Data were analyzed by analysis of variance (ANOVA)

from acetyl-CoA, which is catalyzed by acetyl-CoA carboxylase (*AccB*/*AccC*) (Tao et al. 2016). In bacterial cells, enzymes that play a dominant role in catalyzing fatty acid production are primarily acyl carrier protein polymers (*FabZ2*, *FabG2*, *FabD*, and *FabH*). Acetyl-CoA is catalyzed by Fab to obtain long-chain fatty acyl-ACP, which then enters the phospholipid synthesis pathway. In the present study, *AccB*, *FabZ2*, *FabG2*, and *FabD* were repressed in *L. plantarum* FS5-5 in response to 6.0, 7.0, and 8.0% (*w*/*v*) NaCl stress but remained unaltered in response to low salt stress. This result indicated that high salt stress inhibited the synthesis of phospholipids in *L. plantarum* FS5-5 and damaged the formation of cell membranes. *L. plantarum* FS5-5 could not resist osmotic stress to maintain the normal growth of cells through this pathway. Similar results have been observed in a previous study by Heunis et al. (2014), who observed a marked decrease in proteins playing a role in fatty acid biosynthesis in *L. plantarum* 423 under acid stress. We speculate the reason for these results may be that fatty acid metabolism in *L. plantarum* was inefficient in resisting environmental stress.

Proteins involved in nucleotide metabolism

Purine and pyrimidine metabolism were also affected by salt stress; the expression of purine and pyrimidine metabolic enzymes was significantly downregulated under salt stress.

GuaC, *PurH*, *PurA*, and *PurB* are involved in purine metabolism. *GuaC* is a key enzyme that catalyzes the production of IMP (hypoxanthine nucleotide) by GMP (guanine nucleotide). *PurH* and *PurB* are key enzymes that catalyze the production of IMP by GAR (5′-phosphoribosyl-glycinamide). *PurA* is a key enzyme that catalyzes IMP to produce AMP (adenosine monophosphate); GMP, IMP, and AMP are precursors for cellular nucleic acid synthesis. In this study, the expressions of *GuaC*, *purH*, *PurA*, and *PurB* were downregulated under salt stress. This result indicated that under salt stress, the purine metabolic process of *L. plantarum* FS5-5 was disrupted, Moreover, the generation of precursors for nucleic acid synthesis was reduced, which blocked the synthesis of DNA and RNA in cells, and this may be a reason for the slow growth of cells under salt stress. Similar to our results, *PurH* and *PurB* of *L. rhamnosus* GG were downregulated in response to acid stress (Koponen et al. 2012). Conversely, it has been reported that the expressions of *PurA* and *PurH* are upregulated in *L. sakei* CRL1756 and in *L. lactis* SK11 under salt stress (Zhang et al. 2010; Belfiore et al. 2013). These contrasting results may indicate that modified purine metabolism may be strain-specific, and for *L. plantarum* FS5-5, purine metabolism may be unnecessary or inefficient in resisting salt stress.

CarA (carbamoyl-phosphate synthase small subunit), *PyrE* (orotate phosphoribosyltransferase), and *PyrF* (orotidine-5′-phosphate decarboxylase) were downregulated in response to all salt stress conditions, and *PyrB* (aspartate carbamoyltransferase catalytic subunit), *PyrC* (dihydroorotase), *PyrD* (dihydroorotate dehydrogenase (fumarate)), *PyrG* (CTP synthase), involved in pyrimidine metabolism, were downregulated in response to high salt stress conditions in the present study. *CarA*, *PyrB*, *PyrC*, *PyrD*, *PyrE*, and *PyrF* are key enzymes in the pathway that catalyzes the formation of UMP (uridine monophosphate) by L-glutamine. *PyrG* is a key enzyme that catalyzes the formation of CTP (cytidine triphosphate) by UTP (uridine triphosphate), and both UTP and CTP are precursors to RNA synthesis. In our study, downregulation of these enzymes indicated that the synthesis of pyrimidines in *L. plantarum* FS5-5 was blocked under salt stress, thus, tampering with RNA synthesis. A previous study has shown that the abundance of pyrimidine and purine biosynthesis enzymes in *L. rhamnosus* GG is highly reduced in response to lower pH condition (Koponen et al. 2012). These results may be due to the fact that the pyrimidine synthesis system is susceptible to damage under environmental stress, which impedes RNA synthesis in cells, and this may also be one of the reasons for the slow growth of cells under environmental stress.

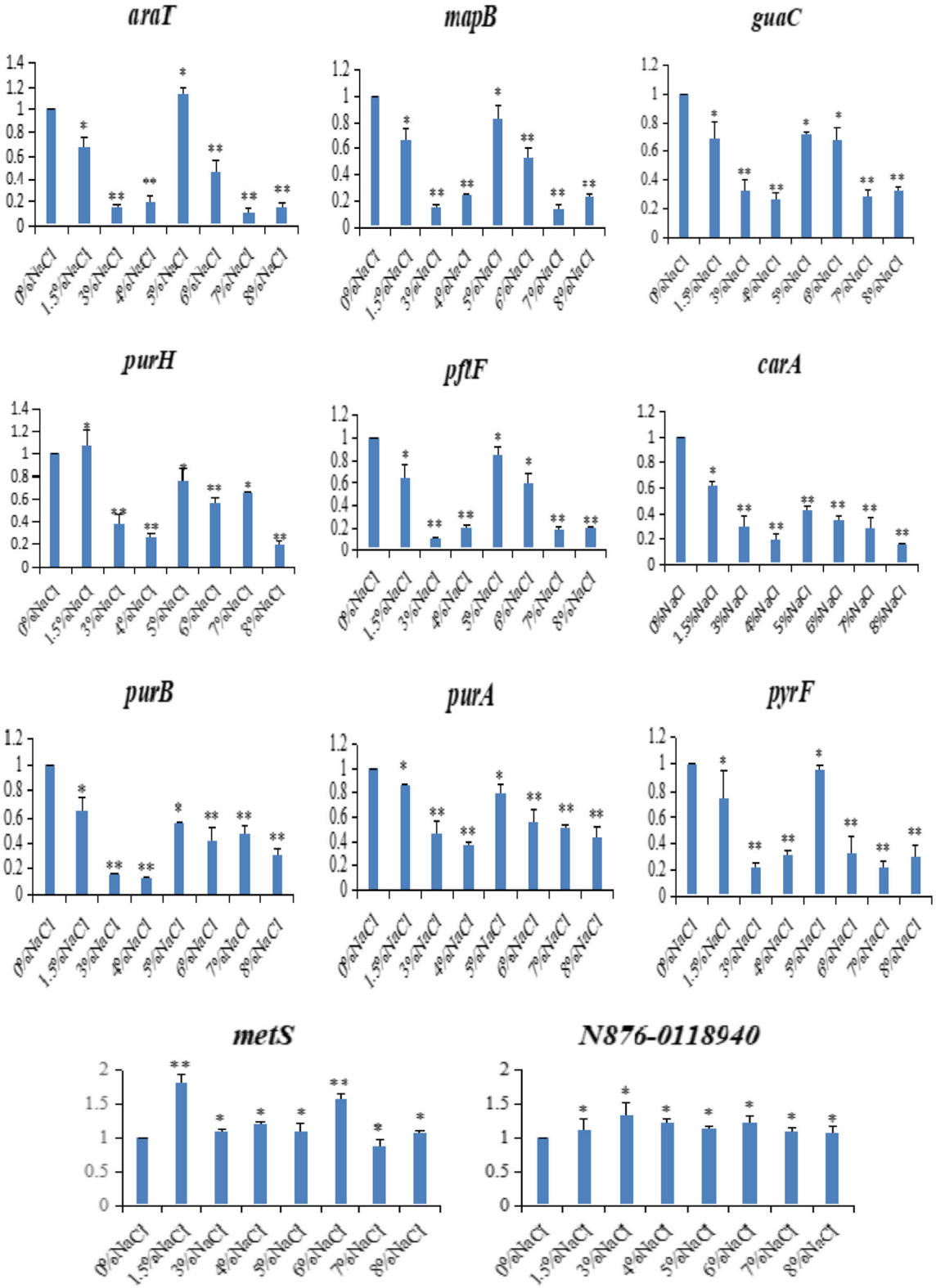

Fig. 5 Trend graph of corresponding gene transcriptional expression by qRT-PCR analysis in *Lactobacillus plantarum* FS5-5 cells after being exposed to 0% NaCl, 1.5% (*w*/*v*) NaCl, 2.0% (*w*/*v*) NaCl, 3.0% (*w*/*v*) NaCl, 4.0% (*w*/*v*) NaCl, 5.0% (*w*/*v*) NaCl, 6.0% (*w*/*v*) NaCl, 7.0% (*w*/*v*) NaCl, or 8.0% (*w*/*v*) NaCl. The x-axis represents the gene transcription of *Lactobacillus plantarum* FS5-5 cultivated in MRS at 0% (*w*/*v*) NaCl (control) or 1.5% (*w*/*v*) NaCl, 3.0% (*w*/*v*) NaCl, 4.0% (*w*/*v*) NaCl, 5.0% (*w*/*v*) NaCl (low salt stress), 6.0% (*w*/*v*) NaCl, 7.0% (*w*/*v*) NaCl, 8.0% (*w*/*v*) NaCl (high salt stress), and the y-axis represents the normalized fold expression of genes. Error bars represent the SD of three independent experiments, and the asterisks indicate a significant difference (*$P < 0.05$, **$P < 0.01$)

Proteins involved in peptidoglycan biosynthesis

MurA (UDP-N-acetylglucosamine 1-carboxyvinyltransferase) and *MurB* (UDP-N-acetylmuramate dehydrogenase) are involved in the peptidoglycan biosynthesis pathway, wherein monomers are utilized for peptidoglycan biosynthesis. Previous reports have reported that peptidoglycan biosynthesis-related enzymes are inhibited in *L. fermentum* NCDC 400 under salt stress and in *L. johnsonii* PF01 under bile salt stress (Lee et al. 2013; Kaur et al. 2017). These enzymes are a part of the more complex amino–sugar metabolic pathway that consumes energy and may be unnecessary and inefficient for cells coping with a harsh environment.

Ribosomal, transporter, DNA repair, and stress proteins

Ribosomal proteins are the main components of the ribosome and play an important role in the biosynthesis of proteins in cells. In our study, the expressions of *rpsL* (*30S ribosomal protein S12*), *rpmA* (*50S ribosomal protein L27*), *rpmI* (*50S ribosomal protein L35*), *rpsT* (*30S ribosomal protein S20*), *rpmB* (*50S ribosomal protein L28*), *rplO* (*50S ribosomal protein L15*), and *rplB* (*50S ribosomal protein L2*) were downregulated by high salt stress but remained unaltered in response to low salt stress. These downregulated genes comprise regulatory genes involved in replication, transcription, and translation. Under high salt stress, the expression of these genes was significantly inhibited, indicating that the rate of protein synthesis in *L. plantarum* FS5-5 decreased under high salt stress, thus, inhibiting cell growth. Previous studies have shown that *ribosomal protein L10* is downregulated by acid stress (Wu et al. 2011), and ribosomal proteins are sensitive to cold and heat shock (Jones et al. 1996). The results of the present study imply that ribosomal proteins in *L. plantarum* FS5-5 were also highly sensitive to salt stress and did not play an active role in response to salt stress.

OpuA (osmoprotectant transport system ATP-binding protein) is a compatible transporter belonging to GB (glycine betaine) transport systems. GB, as one of the most universal and effective osmoprotectants, is accumulated by bacteria (Considine et al. 2011). *OpuA* expression was highly upregulated under higher concentrations of NaCl, which may indicate that *L. plantarum* FS5-5 utilized the compatible solute regulatory system to sustain its growth. The change in *OpuA* expression confirmed that the compatible solute regulatory system is one of the mechanisms of *L. plantarum* FS5-5 in response to salt stress. Expression of ABC transporter proteins increased in *L. plantarum* FS5-5 under high salt stress but remained unaltered in response to low salt stress in this study, which may indicate that the cells require ABC transporter to maintain the balance of osmotic pressure under high salt stress. A previous study has reported that ABC transporter *LmrCD* is the major transporter responsible for bile acid resistance in *L. lactis* (Zaidi et al. 2008).

Damage repair seems to be the ultimate mechanism of resistance against oxidative and other stresses. High salt stress triggered upregulation of genes encoding DNA repair proteins, including *uvrB* and *recA*, in *L. plantarum* FS5-5. Similarly, the expression of DNA repair proteins has been reported to be upregulated in *L. plantarum* ST-III under salt stress (Zhao et al. 2014). This upregulation indicated that DNA repair is an essential strategy for *L. plantarum* to adapt to high salt environments.

Stress proteins play an important role in protein expression and repair. In this study, the expressions of universal stress protein, small heat shock protein, alkaline shock protein, and general stress protein were increased by high salt stress. In response to salt stress, osmotic pressure caused high plasmolysis and reduced water activity, leading to the accumulation of denatured proteins, which in turn induced a stress protein regulation system to protect proteins and macromolecules in the cells and to prevent cell damage caused by salt stress.

Conclusions

In present study, we reported the proteomics of salt-tolerant *L. plantarum* at different salt concentrations. The response of *L. plantarum* to increased salt concentration is likely complex, involving a combination of different metabolic pathways. Dramatic changes were observed in amino acid, carbohydrate, nucleotide, and lipid metabolism; ABC transporter; ribosomal protein; replication and repair; and PTS. The gene expression of *N876_0118940*, involved in peptidoglycan hydrolysis, and *metS*, involved in amino acid metabolism, were upregulated in cells at all NaCl levels. *GshAB*, *GshR3*, *PepN*, *GshR4*, and *serA*, involved in amino acid metabolism, and *I526_2330*, *Gpd*, and *Gnd*, involved in carbohydrate metabolism, were upregulated in cells at high NaCl levels. We found that *L. plantarum* FS5-5 needed to initiate more stress responses, including maintaining intracellular and extracellular osmotic pressure balance by increasing the concentration of similar compatible solutes, reducing cell damage under osmotic stress by increasing GSH content, repairing DNA damage by increasing DNA repair protein expression, and priming stress proteins to protect proteins and macromolecules in cells, to prevent cell damage caused by salt stress and to resist high salt stress compared with low salt stress. Moreover, we speculate that *N876_0118940*, *metS*, *GshAB*, *GshR3*, *PepN*, *GshR4*, *serA*, *I526_2330*, *Gpd*, and *Gnd* are closely related to the salt-tolerance mechanism of *L. plantarum* FS5-5 and need to be studied further. The results of the present study provide some new and relevant information on proteomic changes that occur in *L. plantarum* FS5-5 in response to salt stress and sheds light on the adaptive process for different salt

concentrations. In later studies, specific molecular pathways involved in mediating the adaptive response to salt shock stress should be further identified.

Funding This work was financially supported by Natural Science Foundation of China (Grant No.31471713, 31470538, 31000805),Program for Liaoning Excellent Talents in University (Grant No.LR2015059, LjQ2015103), Shenyang Agricultural University Tianzhushan Scholar program.

References

Behera SS, Ray RC, Zdolec N (2018) *Lactobacillus plantarum* with functional properties: an approach to increase safety and shelf-life of fermented foods. Biomed Res Int 2018:1–18

Belfiore C, Fadda S, Raya R, Vignolo G (2013) Molecular basis of the adaption of the anchovy isolate *Lactobacillus sakei* CRL1756 to salted environments through a proteomic approach. Food Res Int 54:1334–1341. https://doi.org/10.1016/j.foodres.2012.09.009

Bengoa AA, Llamas MG, Iraporda C, Dueñas MT, Abraham AG, Garrote GL (2018) Impact of growth temperature on exopolysaccharide production and probiotic properties of *Lactobacillus paracasei* strains isolated from kefir grains. Food Microbiol 69:212–218

Braford MM (1976) A rapid and sensitive method for the quantitation of microgram quantities of protein utilizing the principle of protein-dye binding. Anal Biochem 72:248–254

Considine KM, Sleator RD, Kelly AL, Fitzgerald GF, Hill C (2011) A role for proline synthesis and transport in *Listeria monocytogenes* barotolerance. J Appl Microbiol 110:1187–1194

Engelhardt T, Szakmár K, Kiskó G, Mohácsi-Farkas C, Reichart O (2018) Combined effect of NaCl and low temperature on antilisterial bacteriocin production of *Lactobacillus plantarum* ST202Ch. LWT 89:104–109

Feliciano CP, Rivera WL (2016) Data on preparation of psychrotolerant bacterium *Shewanella olleyana* sp. nov. cells for transmission electron microscopy. Data in Brief 9(C):710–715. https://doi.org/10.1016/j.dib.2016.09.049

Gao K, Deng X, Shang M, Qin G, Hou C, Guo X (2017) iTRAQ-based quantitative proteomic analysis of midgut in silkworm infected with Bombyx mori cytoplasmic polyhedrosis virus. J Proteome 152:300–311

Gill HS, Rutherfurd KJ, Prasad J (2000) Enhancement of natural and acquired immunity by *Lactobacillus rhamnosus* (HN001), *Lactobacillus acidophilus* (HN017) and *Bifidobacterium lactis* (HN019). Br J Nutr 83(2):167–176

Heunis T, Deane S, Smit S, Dicks LM (2014) Proteomic profiling of the acid stress response in *Lactobacillus plantarum* 423. J Proteome Res 13(9):4028–4039

Jones PG, Mitta M, Kim Y, Jiang W, Inouye M (1996) Cold shock induces a major ribosomal-associated protein that unwinds double-stranded RNA in *Escherichia coli*. Proc Natl Acad Sci U S A 87: 5589–5593

Jones ML, Martoni CJ, Parent M, Prakash S (2012) Cholesterol-lowering efficacy of a microencapsulated bile salt hydrolase-active *Lactobacillus reuteri* NCIMB 30242 yoghurt formulation in hypercholesterolaemic adults. Br J Nutr 107(10):1505–1513

Kaur G, Alia SA, Kumar S, Mohanty AK, Behare P (2017) Label-free quantitative proteomic analysis of *Lactobacillus fermentum* NCDC 400 during bile salt exposure. J Proteome 167(7):36–45

Kleerebezem M, Boekhorst J, Kranenburg R, Molenaar D, Kuipers OP, Leer R, Tarchini R, Peters SA, Sandbrink HM, Fiers MW, Stiekema W, Lankhorst RM, Bron PA, Hoffer SM, Groot MN, Kerkhoven R, Vries M, Ursing B, Vos WM, Siezen RJ (2003) Complete genome sequence of *Lactobacillus plantarum* WCFS1. Proc Natl Acad Sci 100(4):1990–1995

Koponen J, Laakso K, Koskenniemi K, Kankainen M, Savijoki K, Nyman TA, Vos WM, Tynkkynen S, Kalkkinen N, Varmanen P (2012) Effect of acid stress on protein expression and phosphorylation in *Lactobacillus rhamnosus* GG. J Proteome 75(4):1357

Kovářová J, Barrett MP (2016) The pentose phosphate pathway in parasitic trypanosomatids. Trends Parasitol 32(8):622–634 https://doi.org/10.1016/j.pt.2016.04.010

Lee JY, Pajarillo EA, Kim MJ, Chae JP, Kang DK (2013) Proteomic and transcriptional analysis of *Lactobacillus johnsonii* PF01 during bile salt exposure by iTRAQ shotgun proteomics and quantitative RT-PCR. J Proteome Res 12:432–443

Li C, Liu L, Sun D, Chen J, Liu N (2012) Response of osmotic adjustment of *Lactobacillus bulgaricus* to NaCl stress. Journal of Northeast Agricultural University (English Edition) 19:66–74

Li JY, Jin MM, Meng J, Gao SM, Lu RR (2013) Exopolysaccharide from *Lactobacillus planterum* LP6: antioxidation and the effect on oxidative stress. Carbohydr Polym 98(1):1147–1152

Li J, Liu X, Xiang Y, Ding X, Wang T, Liu Y, Yin M, Tan C, Deng F, Chen L (2017a) Alpha-2-macroglobulin and heparin cofactor II and the vulnerability of carotid atherosclerotic plaques:An iTRAQ-based analysis. Biochem Biophys Res Commun 483:964–971

Li M, Zhang K, Long R, Sun Y, Kang J, Zhang T, Cao S (2017b) iTRAQ-based comparative proteomic analysis reveals tissue-specific and novel ealy-stage molecular mechanisms of salt stress response in *Carex rigescens*. Environ Exp Bot 143:99–114

Lin J, Wu Y, Han B, Chen Y, Wang L, Li X, Liu M, Huang J (2017) iTRAQ-based proteomic profiling of granulosa cells from lamb and ewe after superstimulation. Theriogenology 101:99–108

Livak KJ, Schmittgen TD (2001) Analysis of relative gene expression data using real-time quantitative PCR and the $2^{-\Delta\Delta CT}$ method. Methods 25:402–408

Padan E, Bibi E, Ito M, Krulwich T (2005) Alkaline pH homeostasis in bacteria: new insights. Biochim Biophys Acta (BBA)-Biomembr 1717(2):67–88

Roberts MF (2005) Organic compatible solutes of halotolerant and halophilic microorganisms. Saline Systems 1(1):5. https://doi.org/10.1186/1746-1448-1-5

Romeo Y, Bouvier J, Gutierrez C (2001) Osmotic stress response of lactic acid bacteria *Lactococcus lactis* and *Lactobacillus plantarum* (mini-revue). Lait 81:49–55

Shi S, Chen T, Zhang Z, Chen X, Zhao X (2009) Transcriptome analysis guided metabolic engineering of *Bacillus subtilis* for riboflavin production. Metab Eng 11:243–252

Song X, Wang Q, Xu X, Lin J, Wang X, Xue Y, Wu R, An Y (2016) Isolation and analysis of salt response of *Lactobacillus plantarum* FS5-5 from *Dajiang*. Indian J Microbiol 56(4):1–10

Tao H, Zhang Y, Cao X, Deng Z, Liu T (2016) Absolute quantification of proteins in the fatty acid biosynthetic pathway using protein standard absolute quantification. Synth Syst Biotechnol (3):150–157

Veith N, FeldmanSalit A, Cojocaru V, Henrich S, Kummer U, Wade RC (2017) Organism-adapted specificity of the allosteric regulation of pyruvate kinase in lactic acid bacteria. PLoS Comput Biol 9(7):1–15

Wang DH (2015) Glutathione is involved in physiological response of *Candida utilis* to acid stress. Appl Microbiol Biotechnol 99(24): 10669–10679

Wang Y, Chen C, Ai L, Zhou F, Zhou Z, Wang L, Zhang H, Chen W, Guo B (2011) Complete genome sequence of the probiotic *Lactobacillus plantarum* ST-III. J Bacteriol 193(1):313–314

Wu R, Zhang W, Sun T, Wu J, Yue X, Meng H, Zhang H (2011) Proteomic analysis of response of a new probiotic bacterium

Lactobacillus casei Zhang to low acid stress. Int J Food Microbiol 147:181–187

Wu R, Song X, Liu Q, Ma D, Xu F, Wang Q, Tang X, Wu J (2016) Gene expression of *Lactobacillus plantarum* FS5-5 in response to salt stress. Ann Microbiol 66:1181–1188

Xia K, Zang N, Zhang J, Zhang H, Li Y, Liu Y, Feng W, Liang X (2016) New insights into the mechanisms of acetic acid resistance in Acetobacter pasteurianus using iTRAQ-dependent quantitative proteomic analysis. Int J Food Microbiol 238:241–251

Yang X, Zhang Z, Gu T, Dong M, Peng Q, Bai L, Li Y (2017) Quantitative proteomics reveals ecological fitness cost of multi-herbicide resistant barnyardgrass (*Echinochloa crus-galli* L.). J Proteome 150(6):160–169

Yu H, Wang X, Xu J, Ma Y, Zhang S, Yu D, Fei D, Muhammad A (2017) iTRAQ-based quantitative proteomics analysis of molecular mechanisms associated with *Bombyx mori* (Lepidoptera) larval midgut response to BmNPV in susceptible and near-isogenic strains. J Proteome 165:35–50

Zaidi AH, Bakkes PJ, Lubelski J, Agustiandari H, Kuipers OP, Driessen AJ (2008) The ABC-type multidrug resistance transporter LmrCD is responsible for an extrusion-based mechanism of bile acid resistance in *Lactococcus lactis*. J Bacteriol 190(22):7357–7366

Zhang Y, Zhang Y, Zhu Y, Mao S, Li Y (2010) Proteomic analyses to reveal the protective role of glutathione in resistance of *Lactococcus lactis* to osmotic stress. Appl Environ Microbiol 76(10):3177–3186

Zhao S, Zhang Q, Hao G, Liu X, Zhao J, Chen Y, Zhang H, Chen W (2014) The protective role of glycine betaine in *Lactobaciluus plantarum* ST-III against salt stress. Food Control 44:208–213

Zou X, Feng Z, Li Y, Wang Y, Wertz K, Weber P, Yan F, Liu J (2014) Stimulation of GSH synthesis to prevent oxidative stress-induced apoptosis by hydroxytyrosol in human retinal pigment epithelial cells: activation of Nrf2 and JNK-p62/SQSTM1 pathways. J Nutr Biochem 78(8):70–78